Photophysics of Entwined Porphyrin Conjugates: Competitive Exciton Annihilation, Energy-Transfer, Electron-Transfer, and Superexchange Processes

Anne M. Brun,[†] Stephen J. Atherton,[†] Anthony Harriman,*[,†] Valérie Heitz,[‡] and Jean-Pierre Sauvage*[,‡]

Contribution from the Center for Fast Kinetics Research, The University of Texas at Austin, Austin, Texas 78712, and Institut de Chimie, Université Louis Pasteur, 67000 Strasbourg, France. *Received October 21, 1991*

Abstract: Bisgold(III) bisporphyrins, in which a 1,10-phenanthroline spacer imposes a constrained geometry, have been synthesized. Flash photolysis studies indicate that, at high laser intensity, triplet exciton annihilation occurs with a diffusion coefficient of 4×10^{-5} cm^2 s^{-1}. Two such molecules coordinate to a copper(I) ion, via the 1,10-phenanthroline spacers, to form a tetrameric porphyrin ensemble in which triplet exciton annihilation competes with electron transfer from the copper(I) complex to a gold porphyrin triplet. A mixed multicomponent array, comprising gold(III) and zinc(II) bisporphyrins covalently-linked to a copper(I) bis(1,10-phenanthroline) complex, undergoes a variety of electron-transfer reactions according to which porphyrin absorbs the photon energy. The copper(I) complex participates in these electron-transfer processes via both direct (redox) and indirect (superexchange) mechanisms.

Electron transfer in biological molecules takes place rapidly over long distances (>10 Å) between nonconjugated molecular components. In attempting to understand and to mimic such processes, many elaborate donor–acceptor systems have been studied by laser spectroscopic and pulse radiolytic techniques.[1] However, a proper understanding of electronic coupling between remote donor and acceptor subunits demands the use of well-defined molecular structures in which both separation distance and mutual orientation of the reactants are fixed. A further complication can arise when using biologically-important redox couples, such as metalloporphyrins, and this concerns the difficulty of ensuring selective and monophotonic excitation of the preferred chromophore.[2] We describe here a simple strategy for *assembling clusters of metalloporphyrins which demonstrate rapid photoinduced energy- and/or electron-transfer processes* under illumination at low light intensity. *Several photons can be accommodated on a single cluster*, and, under such conditions, exciton annihilation dissipates part of the photon energy. It is further shown that *the bridging unit can catalyze forward electron transfers between porphyrinic subunits* without affecting the reverse processes. In such respects, these model systems resemble the natural photosynthetic apparatus.[3]

Our approach for constructing organized porphyrin ensembles follows the templated synthesis employed previously to prepare a family of catenands and catenates using complexes with entwined ligands as intermediates.[4] Thus, oblique symmetrical bisporphyrins containing a 1,10-phenanthroline spacer group have been produced[5] with either gold(III) or zinc(II) cations (or two protons) inserted into each porphyrin cavity. This arrangement[6] holds the porphyrin rings at an average center-to-center separation distance of 13.4 Å and an approximate interplanar angle of 77°. Two such 1,10-phenanthroline ligands coordinate to a single copper(I) cation to form a stable tetrahedral complex,[5] the geometry of which positions four identical metalloporphyrins in close proximity around a central copper(I) bis(1,10-phenanthroline) complex (reaction 1). By using asymmetrical bisporphyrins, it

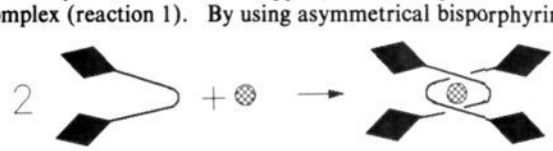

(1)

becomes possible to assemble mixed porphyrin tetramers, although ligands coordinated to the cation at the center of the porphyrin ring may cause a distorted tetrahedral geometry. This strategy generates enantiomers (reaction 2).

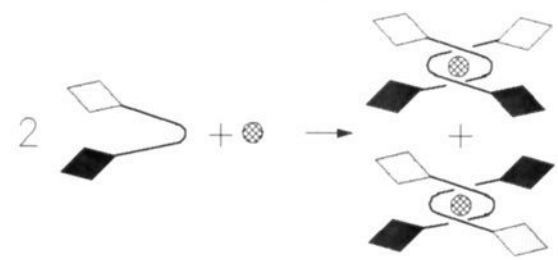

(2)

The present study is an extension of earlier work[1,7] which described the photochemistry of the asymmetrical 1,10-phenanthroline-bridged bisporphyrins prior to their complexation with copper(I). Many related bisporphyrins have been studied under conditions of monophotonic excitation, but little attention has been paid to multiphoton excitation of such systems.[2] It is shown that the central copper(I) complex plays an active role in the photochemistry of the assembled multicomponent systems, in addition to anchoring the porphyrins. *This is the first example of a model system in which a noncovalently-linked molecule may catalyze specific electron-transfer processes*, possibly resembling the role played by the accessory bacteriochlorophyll in reaction centers of photosynthetic bacteria.[3b]

Experimental Section

N,N-Dimethylformamide (DMF) (Aldrich spectroscopic grade) was fractionally distilled from CaH_2. Structures of compounds **1-9** are given

[†] The University of Texas at Austin.
[‡] Université Louis Pasteur.

(1) Brun, A. M.; Harriman, A.; Heitz, V.; Sauvage, J.-P. *J. Am. Chem. Soc.* **1991**, *113*, 8658.
(2) Harriman, A. In *Proceedings 29th Yamada Conference (Osaka)*; Mataga, N., Okada, T., Masuhara, H., Eds.; Elsevier: Amsterdam, 1991.
(3) (a) Mauzerall, D. In *Biological Events Probed by Ultrafast Laser Spectroscopy*; Alfano, R. R., Ed.; Academic Press: New York, 1982; p 215. (b) Bixon, M.; Jortner, J.; Michel-Beyerle, M. E.; Ogrodnik, A.; Lersch, W. *Chem. Phys. Lett.* **1987**, *140*, 626.
(4) (a) Dietrich-Buchecker, C. O.; Sauvage, J.-P.; Kern, J.-M. *J. Am. Chem. Soc.* **1984**, *106*, 3043. (b) Cesario, M.; Dietrich-Buchecker, C. O.; Guilhem, J.; Pascard, C.; Sauvage, J.-P. *J. Chem. Soc., Chem. Commun.* **1985**, 244. (c) Albrecht-Gary, A. M.; Saad, Z.; Dietrich-Buchecker, C. O.; Sauvage, J.-P. *J. Am. Chem. Soc.* **1985**, *107*, 3205.
(5) Heitz, V.; Chardon-Noblat, S.; Sauvage, J.-P. *Tetrahedron Lett.* **1991**, *32*, 197.
(6) Chardon-Noblat, S.; Guilhem, J.; Mathis, P.; Pascard, C.; Sauvage, J.-P. In *Photoconversion Processes for Energy and Chemicals*; Hall, D. O., Grassi, G., Eds.; Elsevier: London, 1989; p 90.
(7) (a) Chardon-Noblat, S.; Sauvage, J.-P.; Mathis, P. *Angew. Chem., Int. Ed. Engl.* **1989**, *28*, 593. (b) Chardon-Noblat, S.; Sauvage, J.-P. *Tetrahedron* **1991**, *47*, 5123.

0002-7863/92/1514-4632$03.00/0

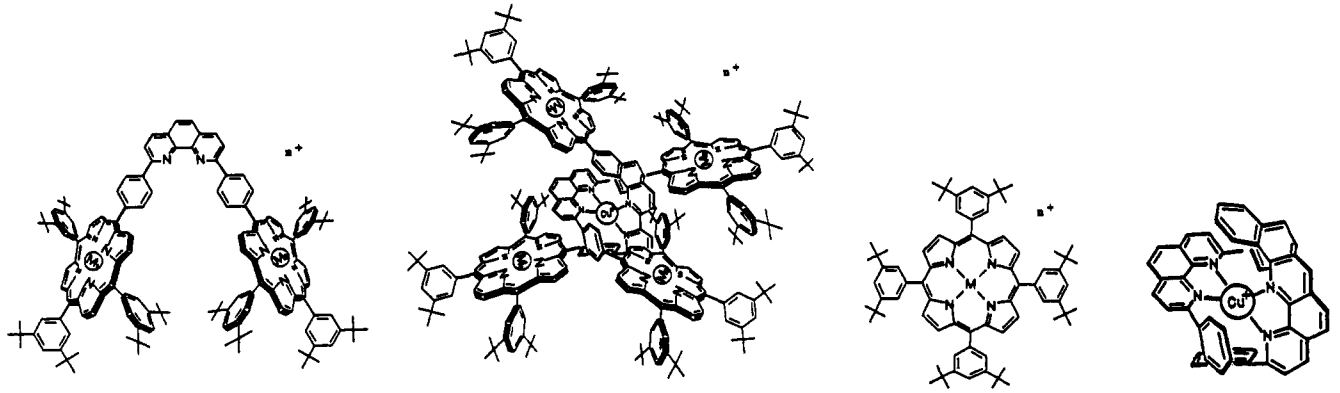

1: $M_1 = M_2 = 2H$: n = 0
2: M_1 = Au: $M_2 = 2H$: n = 1
3: $M_1 = M_2$ = Au: n = 2
4: M_1 = Au: M_2 = Zn: n = 1

5: $M_1 = M_2$ = Au: n = 5
6: M_1 = Au: M_2 = Zn: n = 3

7: M = Au: n = 1
8: M = Zn: n = 0

9

Figure 1. Structures of the compounds used in this study.

in Figure 1. Compound **2** was prepared according to a procedure described recently.[5] It contains a gold(III) porphyrin subunit and a free-base porphyrin site which can be metalated with zinc(II) to afford the asymmetrical compound **4**.[5] Compound **3** was obtained from its bis-free-base precusor[7] **1** by metalation with $KAuCl_4$. Synthesis of **7**,[1] **8**,[7] and **9**[8] was by literature methods. Fresh solutions were used for all experiments since it was found that **6**, in particular, was unstable toward prolonged storage in DMF, even in the dark. The stability appeared to improve following deoxygenation. Absorption spectra recorded before and after the experiment were identical, in each case. All experiments were repeated, at least 3 times, using fresh solutions and performed on different days, and the quoted results are the averages of three or more data sets.

Preparation of the Bisgold(III) Bisporphyrin 3. A mixture of the bis-free-base bisporphyrin **1**[7] (19.8 mg, 9.5 μmol), $KAuCl_4$ (47 μmol), and sodium acetate (76 μmol) in acetic acid (20 mL) was degassed with argon and heated under reflux. The solution gradually turned from green to red. Formation of **3** was monitored by UV–vis spectroscopy and by thin-layer chromatography (TLC). After 2 days of heating, the solvent was pumped off and the residue was dissolved in CH_2Cl_2 before being neutralized by shaking with a 10% aqueous solution of Na_2CO_3. Anion exchange was carried out by stirring the organic phase with a saturated aqueous solution of KPF_6. After the CH_2Cl_2 phase was washed with water and dried over $MgSO_4$, the crude product was purified by column chromatography (SiO_2, CH_2Cl_2 as eluent). Compound **3** was obtained as a red/orange solid in 84% yield. ^1H NMR (CD_2Cl_2) δ: 9.434 (d, 4 H); 9.316 (d, 4 H); 9.302 (s, 8 H); 9.042 (d, 4 H); 8.658 (d, 2 H); 8.588 (d, 2 H); 8.469 (d, 4 H); 8.082 (s, 2 H); 8.039 (d, 4 H); 8.017 (d, 8 H); 7.949 (t, 2 H); 7.911 (t, 4 H); 1.508 (s, 36 H); 1.459 (s, 72 H). FAB-MS (nitrobenzyl alcohol matrix): mol wt calcd for $[3^{2+}, 2PF_6^-]$ = 2758.8; characteristic ion found $[3^{2+}]$ = 1234.3. UV–vis (CH_2Cl_2) λ_{max} (nm) [log ε]: 415 [5.86]; 525 [4.63].

Preparation of the Tetrakisgold(III) Tetrakisporphyrin/Copper(I) Bis(1,10-phenanthroline) Compound 5. To a degassed solution of **3** (22 mg, 8 μmol) in CH_2Cl_2 is added a solution of $Cu(CH_3CN)_4^+ \cdot BF_4^-$ (4.7 μmol) in CH_3CN at room temperature under argon. The solution was agitated on a magnetic stirrer for 3 h at room temperature before being pumped to dryness. The residue was dissolved in CH_2Cl_2, washed with water, and stirred with a saturated aqueous solution of KPF_6. After column chromatography (SiO_2, CH_2Cl_2 as eluent), **5** was obtained as a red/orange solid in 70% yield. ^1H NMR (CD_2Cl_2) δ: 9.399 (d, 8 H); 9.347 (d, 8 H); 9.332 (d, 8 H); 8.949 (d, 8 H); 8.741 (d, 4 H); 8.694 (d, 4 H); 8.691 (d, 8 H); 8.108 (d, 16 H); 8.088 (d, 8 H); 7.978 (t, 4 H); 7.960 (t, 8 H); 7.878 (d, 8 H); 7.435 (s, 4 H); 1.554 (s, 72 H); 1.525 (s, 144 H). ES-MS: mol wt calcd for $[5^{5+}, 5PF_6^-]$ = 5726.1; characteristic ions found $[5^{5+}, 2PF_6^-]$ = 1763.7; $[5^{5+}]$ = 1000.1. UV–vis (CH_2Cl_2) λ_{max} (nm) [log ε]: 262 [4.93]; 303 [5.01]; 417 [6.15]; 525 [4.95].

Preparation of the Bisgold(III) Bisporphyrin/Biszinc(II) Bisporphyrin/Copper(I) Bis(1,10-phenanthroline) Compound 6. To a degassed solution of **4** (28 mg, 11.3 μmol) in CH_2Cl_2 (6 mL) is added a CH_3CN solution (5 mL) of $Cu(CH_3CN)_4^+ \cdot BF_4^-$ (6.8 μmol) under argon. After 3 h of stirring at room temperature, the solvent was pumped off. The crude product was dissolved in CH_2Cl_2, washed with water, and stirred with a saturated aqueous solution of KPF_6. After column chromatography (SiO_2; [CH_2Cl_2 + CH_3OH (0.3–0.5%)] as eluent), some of the starting material **4** was recovered and compound **6** was obtained in 45% yield. ^1H NMR (CD_2Cl_2) δ: 9.359 (d, 4 H); 9.351 (d, 4 H); 9.336 (d, 4 H); 9.024 (d, 4 H); 9.006 (d, 4 H); 8.984 (d, 4 H); 8.837 (d, 4 H); 8.733 (d, 2 H); 8.693 (d, 2 H); 8.671 (d, 2 H); 8.637 (d, 2 H); 8.609 (d, 4 H); 8.548 (d, 4 H); 8.544 (d, 4 H); 8.099 (d, 8 H); 8.095 (d, 8 H); 8.083 (d, 8 H); 7.982 (t, 2 H); 7.948 (t, 4 H); 7.861 (t, 2 H); 7.856 (d, 4 H); 7.832 (t, 4 H); 7.805 (d, 4 H); 7.472 (d, 2 H); 7.441 (d, 2 H); 1.541 (s, 72 H); 1.512 (s, 144 H). ES-MS: mol wt calcd for $[6^{3+}, 3PF_6^-]$ = 5173.0; characteristic ion found $[6^{3+}]$ = 1579.6. UV–vis (CH_2Cl_2) λ_{max} (nm) [log ε]: 306 [4.67]; 421 [5.72]; 526 [4.35]; 551 [4.39]; 590 [3.93].

Absorption spectra in CH_2Cl_2 were recorded with a Kontron-Uvikon 800 and in DMF with a Hitachi U3210 spectrophotometer. Luminescence spectra were recorded with a Perkin-Elmer LS5 spectrofluorometer and were corrected for wavelength responses of the detector.[9] Fluorescence quantum yields were measured relative to zinc tetraphenylporphyrin (ZnTPP) (Φ_f = 0.033).[10] Singlet excited state lifetimes were measured by time-correlated, single photon counting using a mode-locked Nd-YAG laser (Antares 76S) synchronously pumping a cavity-dumped Rhodamine 6G dye laser (Spectra Physics 375B/244). Glass cut-off filters were used to isolate fluorescence from scattered laser light. A Hamamatsu microchannel plate was used to detect emitted photons, for which the instrumental response function had an fwhm of 60 ± 10 ps. Data analyses were made according to O'Connor and Phillips[11] using computer deconvolution to minimize reduced χ^2 parameters. All solutions for fluorescence studies were optically dilute and air-equilibrated.

Flash photolysis studies were made with a frequency-doubled, mode-locked Quantel YG402 Nd-YAG laser (pulse width 30 ps).[12] For some studies, the excitation pulse was Raman-shifted by focusing into a 10-cm path length cell containing perdeuterated cyclohexane. Glass filters were used to isolate the resultant 598-nm pulse. Laser intensities were attenuated with crossed polarizers, and 300 laser shots were averaged for each measurement. Solutions were adjusted to possess absorbances of ca. 0.4 at the excitation wavelength and were purged with N_2. Residual 1064-nm output from the laser was focused into 1/1 D_3PO_4/D_2O to produce a white light continuum for use as the analyzing beam. Variable delay times in the range 0–6 ns were selected in a random sequence, and transient spectra were recorded with an Instruments SA UFS200 spectrograph interfaced to a Tracor Northern 6200 MCA and a microcomputer. Kinetic analyses were made by overlaying about 30 individual

(8) (a) Dietrich-Buchecker, C. O.; Marnot, P. A.; Sauvage, J.-P.; Kirchhoff, J. R.; McMillin, D. R. *J. Chem. Soc., Chem. Commun.* **1983**, 513. (b) Kirchhoff, J. R.; Gamache, Jr., R. E.; Blaskie, M. W.; Del Paggio, A. A.; Lengel, R. K.; McMillin, D. R. *Inorg. Chem.* **1983**, *22*, 2380. (c) Parker, W. L.; Crosby, G. A. *J. Phys. Chem.* **1989**, *93*, 5692.

(9) Argauer, R. J.; White, C. E. *Anal. Chem.* **1964**, *36*, 368.

(10) Egorova, G. D.; Knyukshto, V. N.; Solovev, K. N.; Tsvirko, M. P. *Opt. Spectrosc. USSR* **1980**, *48*, 602.

(11) O'Connor, D. V.; Phillips, D. *Time Resolved Single Photon Counting*; Academic Press: London, 1984.

(12) Atherton, S. J.; Hubig, S. M.; Callen, T.; Duncanson, J. A.; Snowden, P. T.; Rodgers, M. A. J. *J. Phys. Chem.* **1987**, *91*, 3137.

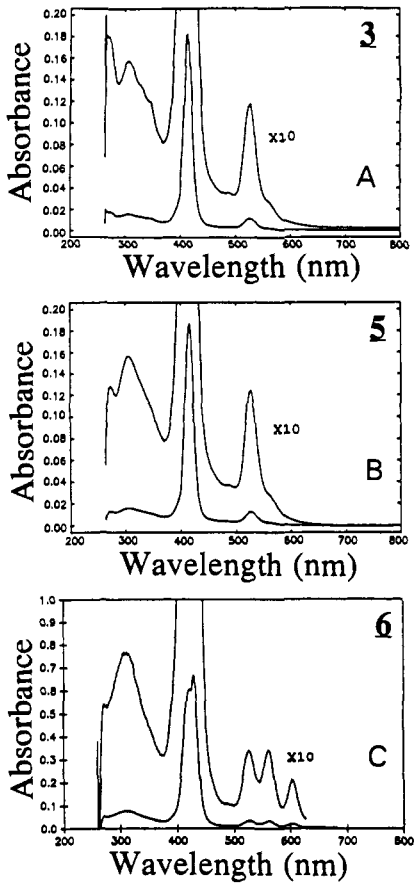

Figure 2. Absorption spectra recorded in DMF solution for (A) 3, (B) 5, and (C) 6.

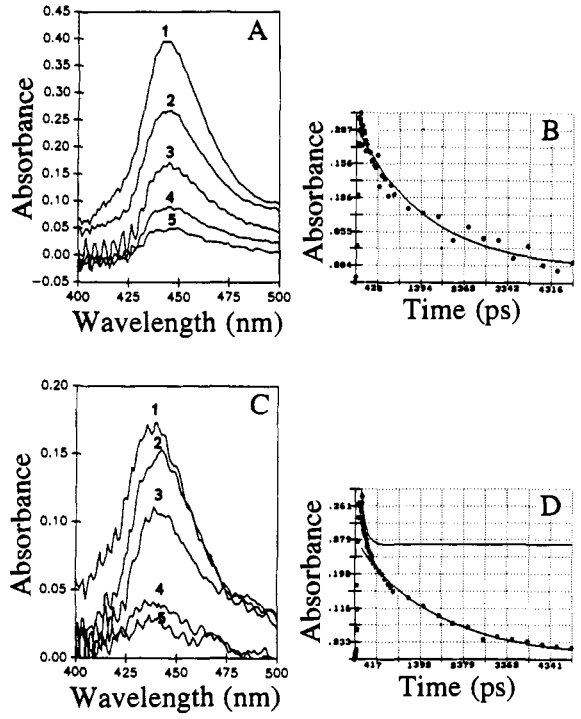

Figure 3. (A) Transient differential absorption spectra recorded after excitation of 3 in DMF with a 2-mJ laser pulse at 532 nm at delay times of (1) 30, (2) 150, (3) 760, (4) 2100, and (5) 3400 ps. (B) Decay profile recorded for the above experiment at 445 nm. (C) Transient differential absorption spectra recorded after excitation of 3 in DMF with a 20-mJ laser pulse at 532 nm at delay times as above. (D) Decay profile observed at 445 nm under conditions described in C.

spectra and fitting data at selected wavelengths using computer nonlinear, least-squares iterative procedures.

Improved time resolution was achieved using a frequency-doubled, mode-locked Antares 76S Nd-YAG laser to pump a Coherent 700 dual-jet (Rhodamine 6G) dye laser operated at 76 MHz. A Quantel Model RGA67-10 regenerative amplifier, a Quantel Model PTA-60 dye laser, and a Continuum SPA1 autocorrelator were used to obtain 3-mJ pulses at 588 nm having a fwhm of ca. 0.7 ps. The spectrometer was run at a frequency of 10 Hz, and data were acquired through a Princeton dual-diode-array spectrograph interfaced to a microcomputer. The detection setup and optical delay line were similar to those used for the 30-ps pulse width experiments except that the exciting and analyzing beams were almost colinear and a polarizing scrambler was inserted into the analyzing beam pathway. Solutions were adjusted to possess absorbances of ca. 0.3 at 588 nm and were purged with N_2.

Electrochemical measurements were made using differential pulse and cyclic voltammetry techniques. The compounds were dissolved in dried DMF containing tetra-*n*-butylammonium perchlorate (0.2 M) and were purged thoroughly with Ar. A Pt microelectrode was used as the working electrode, together with a Pt counter electrode and an SCE reference. The bisgold(III) bisporphyrin 3 undergoes reversible one-electron oxidation and reduction processes, respectively, with half-wave potentials of +1.69 and −0.48 V vs SCE. Comparable values were obtained with the monomeric gold(III) porphyrin 7. For the mixed zinc/gold bisporphyrin 4, additional half-wave potentials of +0.82 and −1.53 V vs SCE were observed and attributed to oxidation and reduction, respectively, of the zinc porphyrin subunit. Copper(I) bis(2,9-diphenyl-1,10-phenanthroline) (9) undergoes reversible one-electron oxidation and reduction processes, respectively, with half-wave potentials of +0.58 and −1.65 V vs SCE in DMF. Oxidation and reduction steps, respectively, are believed to occur at the copper(I) cation and on the ligand. Literature values for the half-wave potential for the oxidation process include +0.69 (CH_3CN),[13] +0.62 (CH_2Cl_2),[14] and +0.56 V vs SCE (H_2O).[15] All redox potentials had a reproducibility of ±20 mV.

Results and Discussion

Photophysical Properties of the Bisgold(III) Bisporphyrin 3. The electronic absorption spectrum recorded for 3 in DMF (Figure 2A) is similar to that of the corresponding monomeric porphyrin 7, and there is no indication of exciton interaction between the two porphyrin rings. Fluorescence is not observed, presumably because the excited singlet state lifetime is shortened due to the internal heavy-atom effect, but weak phosphorescence can be detected in a frozen methanol glass. The phosphorescence maximum occurs at 690 nm, and the spectrum closely resembles that recorded for 7 and for gold(III) tetraphenylporphyrin.[16] The porphyrin excited triplet state differential absorption spectrum matches that recorded for 7 under comparable conditions.[1] Thus, excitation of 3 with a 30-ps laser pulse at 532 nm generates the triplet state which decays via first-order kinetics with a lifetime of 1.5 ± 0.2 ns to re-form the ground-state species (Figure 3A,B). The triplet lifetime is identical to that measured for 7 (τ_t = 1.4 ± 0.2 ns). Direct excitation of the 1,10-phenanthroline subunit at 280 nm does not give fluorescence characteristic of the aryl hydrocarbon, suggesting that rapid electronic energy transfer occurs to the appended porphyrins.[17]

At higher laser intensities, decay of the triplet excited state of 3 becomes biexponential but the spectral profile remains unperturbed (Figure 3C,D). Throughout a wide range of laser intensities (1–25 mJ), the decay profile could be analyzed satisfactorily in terms of two lifetimes of 100 ± 30 ps and 1.5 ± 0.3 ns, with the fractional contribution of the shorter-lived component increasing linearly with increasing laser intensity. These decay profiles were independent of monitoring wavelength. The longer-lived component is attributed to the inherent decay of the gold(III) porphyrin triplet, whereas the shorter-lived component is attributed to intramolecular triplet-triplet annihilation (Scheme I). Since the transient absorption spectral profile is independent of laser intensity, the latter process does not lead to net electron transfer,

(13) Federlin, P.; Kern, J.-M.; Rastegar, A.; Dietrich-Buchecker, C. O.; Marnot, P. A.; Sauvage, J.-P. *New J. Chem.* **1990**, *14*, 9.
(14) Gamache, Jr., R. E.; Rader, R. A.; McMillin, D. R. *J. Am. Chem. Soc.* **1985**, *107*, 1141.
(15) Edel, A.; Marnot, P. A.; Sauvage, J.-P. *Nouv. J. Chim.* **1984**, *8*, 495.
(16) Antipas, A.; Dolphin, D.; Gouterman, M.; Johnson, E. C. *J. Am. Chem. Soc.* **1978**, *100*, 7705.
(17) Davila, J.; Harriman, A. *Tetrahedron* **1989**, *45*, 4737.

Scheme I

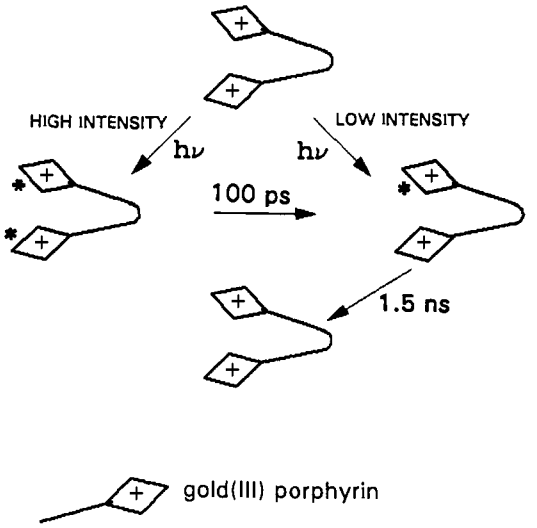

although this is energetically feasible ($\Delta G° = -136$ kJ mol^{-1}),[18] but gives an equimolar mixture of ground and excited singlet states of **3**, the latter rapidly decaying to the exicted triplet state (Scheme I).

The rate constant for intramolecular triplet exciton annihilation ($k_{tt} = 1.0 \times 10^{10}$ s^{-1}) is fast, considering the large amount of energy that must be dissipated as heat (≈138 kJ mol^{-1}), and can be used to derive the exciton diffusion coefficient (D). Taking the porphyrin edge-to-edge separation distance as 9 Å,[6] D has a value of 4×10^{-5} cm^2 s^{-1}. This can be compared to values measured[19] for triplet exciton annihilation in anthracene crystals where $D = 2 \times 10^{-4}$ cm^2 s^{-1}. We are unaware of estimates of D made for any other covalently-linked model system, although long-range triplet annihilation in low-temperature glasses and along polymer chains is well-known.

Photophysics of the Tetrakisgold(III) Tetrakisporphyrin/Copper(I) Bis(1,10-phenanthroline) Compound 5. The absorption spectrum of **5** (Figure 2B) is similar to those of **3** and **7**, and there are no obvious perturbations arising from the presence of the copper(I) complex. The absence of any exciton interaction between chromophores tends to indicate that there are relatively long distances between porphyrinic subunits either borne on the same 1,10-phenanthroline ligand or belonging to two different ligands. Copper(I) bis(2,9-diphenyl-1,10-phenanthroline) (**9**) absorbs weakly at 532 nm ($\epsilon_{532} = 1725$ M^{-1} cm^{-1}), but its contribution to the total absorbance of **5** ($\epsilon_{532} = 21\,700$ M^{-1} cm^{-1}) at this excitation wavelength is only ca. 8%. Thus, immediately after excitation of **5** in DMF with a low-intensity (2 mJ), 30-ps laser pulse at 532 nm the observed transient differential absorption spectrum is characteristic of a gold(III) porphyrin triplet excited state (Figure 4A). The transient absorption decays via biexponential kinetics with lifetimes of 170 ± 20 ps and 2.0 ± 0.4 ns (Figure 4B), even at very low laser intensities. Absorption spectra recorded at different times during the decay process undergo a definite change in profile (Figure 4A). This change is consistent with the triplet state being converted into the gold(III) porphyrin neutral radical.[1] As the laser intensity is increased (Figure 4C), the fractional contribution of the shorter-lived component increases and, whereas the longer lifetime remains unaffected, the shorter lifetime appears to decrease progressively. At the highest laser intensity (25 mJ), the shorter-lived component has a lifetime of ca. 110 ps and accounts for ca. 40% of the initial absorbance at 440 nm (Figure 4D).

The dual-exponential behavior is apparent at the lowest laser intensity (≈0.5 mJ) and well below the onset threshold at which

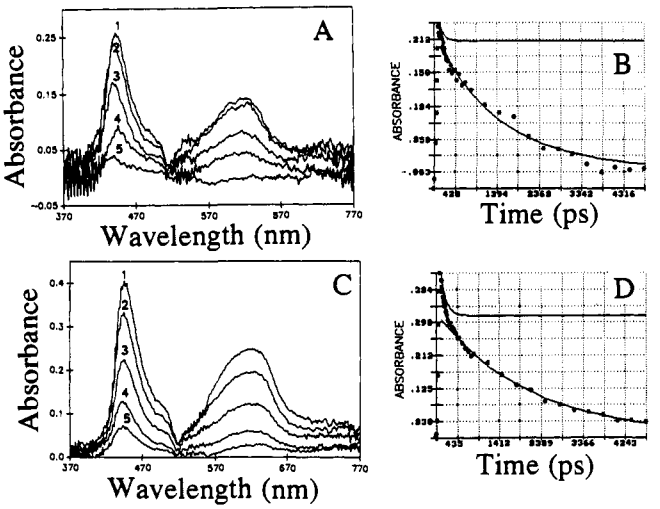

Figure 4. (A) Transient differential absorption spectra recorded after excitation of **5** in DMF with a 1-mJ laser pulse at 532 nm at delay times of (1) 30, (2) 150, (3) 760, (4) 2100, and (5) 3400 ps. (B) Decay profile recorded for the above experiment at 450 nm. (C) Transient differential absorption spectra recorded after excitation of **5** in DMF with a 25-mJ laser pulse at 532 nm at delay times as above. (D) Decay profile observed at 450 nm under conditions described in C.

Scheme II

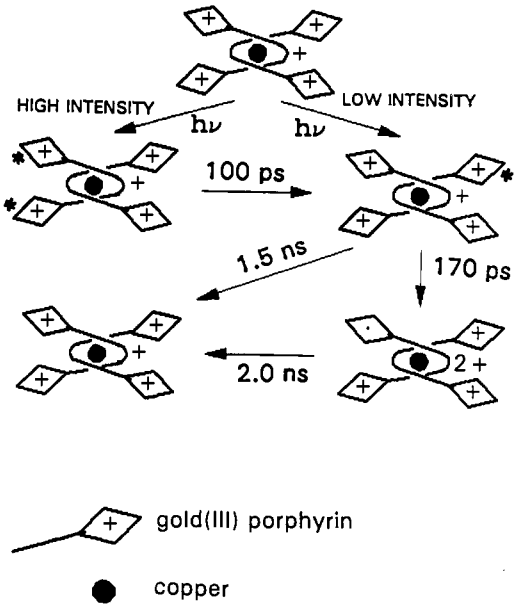

similar behavior becomes apparent for **3**. Although the probability of depositing two photons onto the tetrakisporphyrin ensemble **5** is twice that for the corresponding bisporphyrin **3**, the high concentration and low photon density employed are expected to ensure monophotonic excitation of **5**. Therefore, the dual-exponential decay kinetics observed at low laser intensity are not due to triplet–triplet annihilation but must arise from an additional process.

The thermodynamic driving force for intramolecular electron transfer from the copper(I) complex to the appended gold(III) porphyrin excited triplet state ($\Delta G_{for}°$) in **5** is −70 kJ mol^{-1}.[20] The picosecond laser flash photolysis records could be explained, therefore, in terms of rapid electron transfer from the copper(I) complex to gold porphyrin triplet followed by slower charge recombination (Scheme II). Accepting this model, the rate con-

(18) Calculated as twice the triplet excitation energy (2 × 1.79 eV mol^{-1}) minus the difference between the half-wave potentials for one-electron oxidation and reduction of **3** ($\Delta E = 2.17$ eV mol^{-1}).

(19) Ern, V.; Avakian, P.; Merrifield, R. E. *Phys. Rev.* **1966**, *148*, 862.

(20) Calculated according to $-\Delta G_{for}° = E_{red}° - [E_{ox}° - E_t]$ and $-\Delta G_{rev}° = E_{ox}° - E_{red}°$ where $E_{ox}°$ and $E_{red}°$ refer to the half-wave potentials for one-electron oxidation and reduction, respectively, of **9** and **3** in DMF and E_t (=1.79 eV) is the excitation energy of the porphyrin excited triplet state as determined from luminescence spectroscopy.

Table I. Rate Constants and Reaction Exothermicities for the Various Electron Transfer Steps Described for the Multicomponent Systems

compd	reaction	$k/10^8$ s^{-1}	$\Delta G°$, kJ mol^{-1}
5	$*(AuP^+)-Cu^+ \rightarrow (AuP^•)-Cu^{2+}$	58	−70
5	$(AuP^•)-Cu^{2+} \rightarrow (AuP^+)-Cu^+$	5	−102
5	$(AuP^+)-(Cu^+)^* \rightarrow (AuP^•)-Cu^{2+}$		−66
6	$*(ZnP)-Cu^+-(AuP^+) \rightarrow (^{+•}ZnP)-Cu^+-(AuP^•)$	3300	−73
6[a]	$(^{+•}ZnP)-Cu^+-(AuP^•) \rightarrow (ZnP)-Cu^{2+}-(AuP^•)$	50	−23
6[b]	$(^{+•}ZnP)-Cu^+-(AuP^•) \rightarrow (ZnP)-Cu^{2+}-(AuP^•)$	1	−23
6	$(^{+•}ZnP)-Cu^+-(AuP^•) \rightarrow (ZnP)-Cu^+-(AuP^+)$	17	−123
6	$(ZnP)-Cu^{2+}-(AuP^•) \rightarrow (ZnP)-Cu^+-(AuP^+)$	5	−102
6	$(ZnP)-Cu^+-(AuP^+)^* \rightarrow (^{+•}ZnP)-Cu^+-(AuP^•)$	≥330	−47
6	$(ZnP)-Cu^+-(AuP^+)^* \rightarrow (ZnP)-Cu^{2+}-(AuP^•)$		−70
4[c]	$*(ZnP)-(AuP^+) \rightarrow (^{+•}ZnP)-(AuP^•)$	182	−82
4	$(^{+•}ZnP)-(AuP^•) \rightarrow (ZnP)-(AuP^+)$	17	117
4	$(ZnP)-(AuP^+)^* \rightarrow (^{+•}ZnP)-(AuP^•)$	65	−59

[a] Singlet-state charge-tranfser state. [b] Triplet-state charge-tranfser state. [c] Data for compound 4 taken from ref 1.

stants for forward (k_{for}) and reverse (k_{rev}) electron transfer, respectively, are 5.9×10^9 and 5.0×10^8 s^{-1} (Table I). Previous studies[21] have shown that copper(I) complexes participate readily in redox processes, having high self-exchange rates[21a] even though the resultant copper(II) complex is coordinatively unsaturated. However, k_{rev} seems to be slow in view of the high thermodynamic driving force ($\Delta G_{rev}° = -102$ kJ mol^{-1})[20] and short edge-to-metal center separation distance (ca. 5 Å).

Copper(I) bis(1,10-phenanthroline) complexes are known to luminesce, and **9** emits very weakly in DMF at room temperature with a lifetime of 130 ± 15 ns. The emission band, which is broad and poorly resolved with a maximum around 710 nm, resembles spectra recorded for **9** in CH_2Cl_2.[22] In DMF solution, excitation of **9** with a 30-ps laser pulse at 532 nm generates a transient species having a spectrum similar to that reported[22] in CH_2Cl_2 and that decays with a lifetime of 125 ± 10 ns. This transient species has been assigned to a d–π^* charge-transfer triplet state.[8] Intramolecular triplet energy transfer is possible, therefore, from a gold(III) porphyrin to the copper(I) complex. The small energy gap ($\Delta E \approx 11$ kJ mol^{-1}) may be offset by the extremely short distance between the reactants. On this basis, the short-lived component observed in the decay records at low laser intensity could be associated with intramolecular triplet energy transfer (reaction 3).

$$*(AuP^+)-Cu^+ \rightarrow (AuP^+)-(Cu^+)^* \quad (3)$$

The small energy gap ensures that the two triplets will be in thermal equilibrium at room temperature; the Boltzmann population of the gold porphyrin triplet is calculated to be 27%. The transient spectra show no indication of a contribution from the copper(I) complex, and the decay profiles recorded at low laser intensity cannot be analyzed satisfactorily in terms of a three-state equilibrium model.[23] It is possible that the triplet state of the copper(I) complex, if formed, transfers an electron to the appended gold(III) porphyrin ($\Delta G° = -66$ kJ mol^{-1})[20] (reaction 4). The

$$(AuP^+)-(Cu^+)^* \rightarrow (AuP^•)-Cu^{2+} \quad (4)$$

rate constant for this process, however, would have to be very fast for us not to detect the triplet as an intermediate species. Consequently, we prefer to adopt the direct electron transfer model (Scheme II).

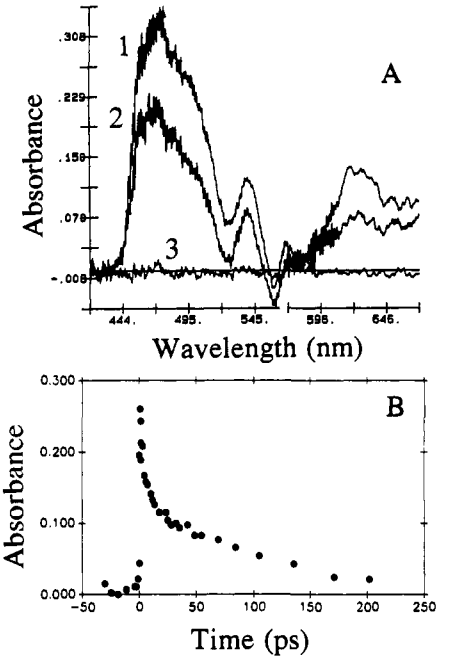

Figure 5. (A) Transient differential absorption spectra recorded after excitation of **6** in DMF with a 0.7-ps laser pulse at 588 nm at delay times of (1) 6 and (2) 20 ps while 3 shows the prepulse baseline; note, the red end of the spectrum is delayed by 3 ps due to spectral chirp. (**B**) Decay profile recorded at 505 nm.

As the laser intensity is increased, the shorter-lived component becomes more pronounced and appears to decay at a faster rate (Figure 4D). Under these conditions, several photons are deposited onto a single molecule of **5** so that the increased significance of the shorter-lived component can be related to the occurrence of triplet–triplet annihilation. The shortening of the lifetime is due to competing triplet annihilation ($k = 1.0 \times 10^{10}$ s^{-1}) and electron transfer ($k = 5.8 \times 10^9$ s^{-1}). At the highest laser intensity (25 mJ), ca. 30% of the absorbed photons are dissipated via exciton annihilation (Scheme II).

Excitation of the Zinc/Gold/Copper Pentad 6 via the Zinc(II) Porphyrin Subunit. The absorption spectrum recorded for **6** in DMF (Figure 2C) appears as a superimposition of spectra of the individual components. Upon excitation at 555 nm, where the zinc porphyrin subunit absorbs >95% of the incident photons, extremely weak fluorescence can be observed. The fluorescence spectrum corresponds to emission from a zinc porphyrin,[1] and the excitation spectrum recorded over the visible region matches that found for **8**. Comparing the fluorescence intensity with that observed for an optically matched, stoichiometric mixture of **7** + **8** + **9** in DMF indicates that the degree of fluorescence quenching in **6** is ca. 99%. The fluorescence lifetime was too short to be separated from the instrument response function by time-correlated single photon counting studies and, therefore, is <20 ps. Of particular interest is the observation that *this extreme fluorescence quenching persists even in an ethanol glass at 77 K.*

Immediately after excitation of **6** with a low-intensity subpicosecond laser pulse at 588 nm, where only the zinc porphyrin subunit absorbs, the characteristic absorption spectral features[24] of the zinc porphyrin excited singlet state were observed (Figure 5A). This species decayed with a lifetime of 3 ± 1 ps[25] to form

(21) (a) Blaskie, M. W.; McMillin, D. R. *Inorg. Chem.* **1980**, *19*, 3519. (b) Palmer, C. E. A.; McMillin, D. R.; Kirmaier, C.; Holten, D. *Inorg. Chem.* **1987**, *26*, 3167.

(22) Bell, S. E. J.; McGarvey, J. J. *Chem. Phys. Lett.* **1986**, *124*, 336.

(23) Heitele, H.; Finckh, P.; Weeren, S.; Pollinger, F.; Michel-Beyerle, M. E. *J. Phys. Chem.* **1989**, *93*, 5173.

(24) Rodriguez, J.; Kirmaier, C.; Holten, D. *J. Am. Chem. Soc.* **1989**, *111*, 6500.

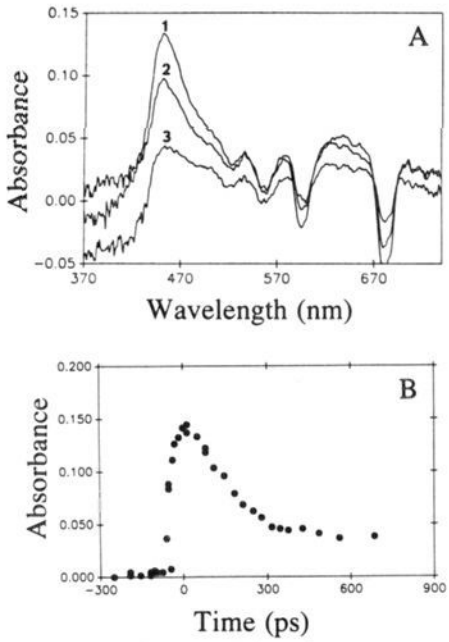

Figure 6. (A) Transient differential absorption spectra recorded after excitation of **6** in DMF with a 30-ps laser pulse (2 mJ) at 598 nm at delay times of (1) 30, (2) 230, and (3) 360 ps. (B) Growth and decay of the zinc porphyrin π-radical cation at 680 nm.

Scheme III

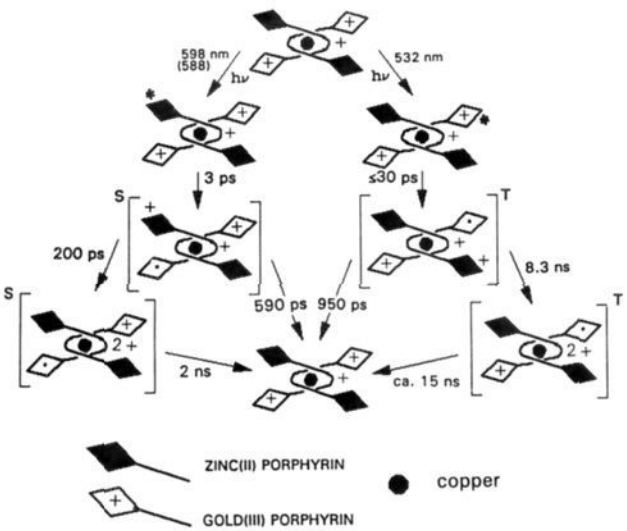

a charge-transfer state[1] (Figure 5) comprising zinc porphyrin π-radical cation and neutral gold(III) porphyrin (Scheme III). There is a thermodynamic driving force of −73 kJ mol^{-1} for this reaction,[26] which occurs with a rate constant of 3.3×10^{11} s^{-1}

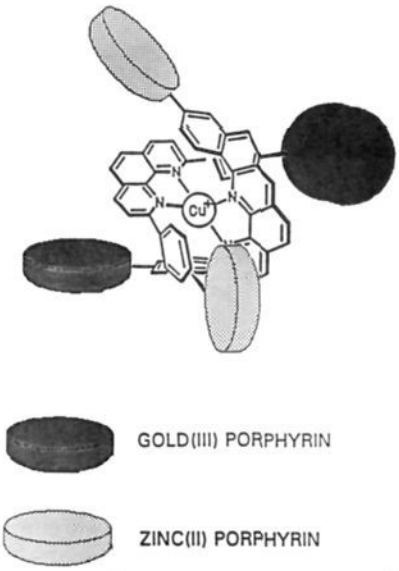

Figure 7. Pictorial representation of the positioning of the accessory 1,10-phenanthroline ligand between the covalently-linked zinc(II) and gold(III) porphyrins.

(Table I). It is interesting to compare this rate constant with that measured previously[1] for electron transfer across the corresponding asymmetrical zinc/gold bisporphyrin **4** ($k = 1.8 \times 10^{10}$ s^{-1}). It appears that the presence of the copper(I) complex enhances the rate of electron transfer by a factor of ca. 18, possibly through a superexchange mechanism[3b,27] or because of structural differences between **4** and **6**. It should be noted, in this context, that earlier work has shown[28] that the rate of electron transfer across asymmetrical bisporphyrins is insensitive toward both separation distance and mutual orientation, supporting a superexchange mechanism in the present case.

Deactivation of the charge-transfer state occurred with a rate constant of 6.7×10^9 s^{-1}, as measured following excitation of **6** with a low-intensity 30-ps laser pulse at 598 nm, to leave a residual transient possessing the characteristic absorption spectrum of a gold(III) porphyrin neutral radical (Figure 6).[1] This decay process may involve rapid intramolecular electron transfer from the copper(I) complex to the zinc porphyrin π-radical cation ($\Delta G°$ = −23 kJ mol^{-1})[26] (reaction 5) or direct reverse electron transfer between the primary products ($\Delta G_{rev}° \approx$ −123 kJ mol^{-1})[26] (reaction 6) (see Scheme III). Assuming that the rate constant for reaction

$$(^{+\bullet}\text{ZnP})\text{–}\text{Cu}^{+}\text{–}(\text{AuP}^{\bullet}) \rightarrow (\text{ZnP})\text{–}\text{Cu}^{2+}\text{–}(\text{AuP}^{\bullet}) \qquad (5)$$

$$(^{+\bullet}\text{ZnP})\text{–}\text{Cu}^{+}\text{–}(\text{AuP}^{\bullet}) \rightarrow (\text{ZnP})\text{–}\text{Cu}^{+}\text{–}(\text{AuP}^{+}) \qquad (6)$$

6 is the same as that measured for the corresponding process in **4** ($k_6 = 1.7 \times 10^9$ s^{-1}), then this reaction accounts for only ca. 25% of the total decay of the zinc porphyrin π-radical cation. Most (i.e., ca. 75%) of the zinc porphyrin π-radical cation, therefore, decays via reaction 5 with a rate constant of 5.0×10^9 s^{-1} (Table I). The residual signal has a lifetime of 2.0 ± 0.4 ns and decays to ground-state **6** (Scheme III). This latter process is attributed to reverse electron transfer between the copper(II) complex and the adjacent gold porphyrin neutral radical (reaction 7), and the derived rate constant is identical to that measured for the corresponding process in **5** (Table I).

$$(\text{ZnP})\text{–}\text{Cu}^{2+}\text{–}(\text{AuP}^{\bullet}) \rightarrow (\text{ZnP})\text{–}\text{Cu}^{+}\text{–}(\text{AuP}^{+}) \qquad (7)$$

It is not possible to distinguish which of the two gold(III) porphyrins within **6** functions as the electron acceptor in the electron transfer process from the excited singlet state of a zinc

(25) Accurate determination of this lifetime is difficult because the decay profiles require analysis in terms of three exponentials but the paucity of data points, together with the restricted time window, preclude such elaborate data fitting. Instead, decay profiles were analyzed over limited time regimes in terms of two exponentials. The derived lifetimes, therefore, were found to be wavelength-dependent, according to the contribution of the third component. The most consistent results were obtained over the wavelength range 480–550 nm, where the gold(III) porphyrin neutral radical shows little absorption. Analysis as two exponentials decaying completely to the original baseline gave lifetimes of 3 ± 1 and 140 ± 25 ps; the longer lifetime was determined to be 150 ± 20 ps by separate experiments using longer time scales. Similar analysis performed over the entire wavelength range gave an average lifetime of 6 ± 3 ps for the shorter-lived species. Stimulated Raman further complicated data analysis, but this decayed with the time profile of the laser pulse and could be deconvoluted from the decay profile.

(26) Calculated as for ref 20 using half-wave potentials measured for **4** and **9** in DMF. No correction was applied for changes in Coulombic potential, due to uncertainty about the correct value for the dielectric constant, so that the quoted value is a lower limit.

(27) Marcus, R. A.; Almeida, R. *J. Phys. Chem.* **1990**, *94*, 2973, 2978.

(28) Osuka, A.; Maruyama, K.; Mataga, N.; Asahi, T.; Yamazaki, I.; Tamai, N. *J. Am. Chem. Soc.* **1990**, *112*, 4958.

porphyrin subunit (reaction 8). The distances between the two sets of donor/acceptor couples may be quite similar, and, in fact, there is no close proximity between porphyrin nuclei within **5** and **6**, as indicated by the absence of exciton interaction. We have

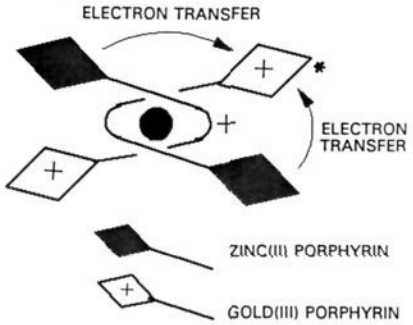

(8)

no means of distinguishing electron transfer processes occurring between covalently-linked porphyrins from those taking place between porphyrinic subunits belonging to two different entwined ligands (see reaction 8). However, it should be noted that the rear of the accessory 1,10-phenanthroline is interspersed between the covalently-linked zinc(II) and gold(III) porphyrins (Figure 7). This ligand, which is an integral part of the copper(I) complex, could act as a bridge for electron transfer between porphyrins linked to the other 1,10-phenanthroline nucleus since it is positioned very close (at an angle of ca. 40°) to each of the porphyrin rings. Thus, the copper(I) complex may facilitate a single-step electron transfer, mediated by superexchange electronic interactions, without appearing as a discrete intermediate.[3b] Also, the close proximity should favor rapid electron transfer from the zinc porphyrin π-radical cation to the copper(I) complex (reaction 5), allowing this reaction to compete with the more thermodynamically favored direct reverse electron transfer (reaction 6).

Excitation of the Zinc/Gold/Copper Pentad 6 via the Gold(III) Porphyrin Subunit. According to control experiments made with the corresponding molecular fragments, the gold(III) porphyrin subunit in **6** absorbs ca. 85% of the incident photons at 532 nm; the remainder partitions between zinc porphyrin (7%) and copper(I) complex (8%). *Phosphorescence from the gold(III) porphyrin subunit could not be detected in an ethanol glass at 77 K*, indicating that extremely efficient quenching occurs in this system. Immediately after excitation of **6** with a low-intensity (2 mJ), 30-ps laser pulse at 532 nm, the characteristic transient differential absorption spectrum of a gold(III) porphyrin triplet state is observed (Figure 8). The triplet decays within the laser pulse, indicating a lifetime $\leq$30 ps, to generate a longer-lived transient whose spectrum corresponds to that characterized as being an equimolar mixture of the gold(III) porphyrin neutral radical and the zinc porphyrin π-radical cation.[1] [From the inflection observed around 590 nm, it is clear that the zinc porphyrin subunit is bleached during the lifetime of this species.] Thus, the primary reaction involves electron transfer between porphyrins (Scheme III). This reaction appears to be favored over electron abstraction from the copper(I) complex (reaction 9). It

$$(ZnP)\text{–}Cu^{+}\text{–}(AuP^{+})^{*} \rightarrow (ZnP)\text{–}Cu^{2+}\text{–}(AuP^{\bullet}) \qquad (9)$$

is also noteworthy that the rate of electron transfer far exceeds that derived for the corresponding process in the asymmetrical bisporphyrin **4** (Table I). Again, this is consistent with the copper(I) complex mediating electron transfer between the porphyrins via a superexchange mechanism[3b,27] or because of a greater proximity between the porphyrinic components involved in the electron-transfer process.

It should be stressed that, because of the spin multiplicity of their precursor excited states, the charge-transfer states produced by excitation of the different porphyrinic subunits differ by virtue of their spin, at least initially. The charge-transfer state produced via excitation into the gold(III) porphyrin subunit must have overall triplet spin (Scheme III). This species decays via first-order kinetics, with a lifetime of 800 $\pm$ 70 ps, to re-form ground-state **6**, although a small amount ($\approx$10%) decays to form a transient

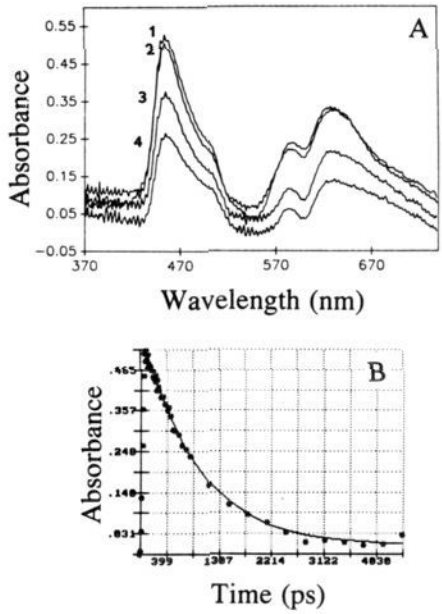

Figure 8. (A) Transient differential absorption spectra recorded after excitation of **6** in DMF with a 30-ps laser pulse (2 mJ) at 532 nm at delay times of (1) 30, (2) 100, (3) 430, and (4) 760 ps. (B) Decay profile recorded at 455 nm.

that survives over several nanoseconds (Figure 8B). The latter species is believed to arise from intramolecular electron transfer from the copper(I) complex to the zinc porphyrin π-radical cation (Scheme III). The rate constant for this process ($k \approx 1.2 \times 10^{8}$ s^{-1}) is much lower than found following direct excitation of the zinc porphyrin subunit, the only difference between the two cases being the spin multiplicity of the charge-transfer state. Thus, preservation of triplet multiplicity appears to cause a marked reduction in the rate of this reaction.

Direct charge recombination occurs with a rate constant (k = 1.1×10^{9} s^{-1}) somewhat lower than that derived for the corresponding process in **4** ($k = 1.7 \times 10^{9}$ s^{-1}). The small difference may reflect slight changes in the geometry of the compounds, but, as found with **4**, the rate of this reaction appears to be insensitive to the overall spin multiplicity. The copper(I) complex does not catalyze this reaction, unlike the forward reactions and, thereby, amplifies the differential between rates of forward and reverse electron transfers.

Concluding Remarks. The molecular systems described here represent interesting, if crude, models for the photosynthetic apparatus[3,27] and demonstrate several noteworthy features: Exciton annihilation occurs at moderate light intensity and competes with photoinduced electron transfer between dissimilar metalloporphyrins. *The copper(I) cation plays a multifarious role and serves to (1) assemble the tetrameric porphyrin ensemble, (2) form a bis(1,10-phenanthroline) complex which catalyzes the forward electron transfer steps, and (3) function as an electron donor.* Indeed, two observations concerning the role of the copper(I) complex demand further attention, namely, (1) why the rates of the forward electron transfer reactions in **6** are enhanced relative to those in **4** but the reverse reactions appear to be unaffected and (2) why the copper(I) complex donates an electron to the zinc porphyrin π-radical cation in a singlet charge-transfer state on a much faster time scale than for the analogous triplet state. These observations have arisien because of the unique molecular architecture achieved with the templated synthetic approach used here, and we expect to explore these effects in more detail. The apparent ability of the copper(I) complex to operate in a unidirectional superexchange mechanism is especially intriguing and will be subjected to further scrutiny. It may be possible, by virtue of synthesizing judicious model systems, to distinguish between a "proximity" effect and a "superexchange" mechanism. Finally, as with the natural photosynthetic system,[3b] very efficient excited-state quenching occurs for **6** at 77 K, and

we expect to describe the temperature dependence of the photochemistry of this compound shortly.

Acknowledgment. Support for this work was provided by the CNRS, the Texas Advanced Research Program, and the National Science Foundation (CHE 9102657). The CFKR is supported jointly by the Division of Research Resources of the NIH (RR00886) and by The University of Texas at Austin. We thank the U.S. Department of Energy for the award of a grant enabling construction of the subpicosecond laser flash spectrometer.

Controlling Solid-State Reaction Mechanisms Using Diffusion Length in Ultrathin-Film Superlattice Composites

Loreli Fister and David C. Johnson*

Contribution from the Department of Chemistry and Materials Science Institute, University of Oregon, Eugene, Oregon 97403. *Received October 21, 1991*

Abstract: The synthetic parameters used by solid-state chemists have essentially been limited to temperature, pressure, composition, and time. Diffusion length can also be used as a synthetic parameter to alter the pathway of a solid-state reaction. Modulated, binary, ultrathin films of similar stoichiometry have been made whose repeat distance varies from 18 to 128 Å. For samples whose modulation length is 38 Å or larger, the films evolve upon heating as thin-film diffusion couples, initially growing an amorphous layer and then crystallizing a stable product, $MoSe_2$, at the interface between individual elemental layers. For samples of 27 Å or smaller, the films evolve to a homogeneous, amorphous alloy before crystallizing $MoSe_2$. This implies a critical layer thickness, below which it is possible to form a homogeneous, amorphous alloy. There is a difference in nucleation temperature of several hundred degrees between the two length scales reflecting the importance of interfaces in aiding nucleation. The synthetic importance of these results—the ability to control synthetic variables to reach desired reaction intermediates in solid-state reactions—is highlighted.

Introduction

Molecular chemistry is based upon the kinetic control of the reaction pathway to obtain kinetic products. *In contrast, this general ability to control the reaction pathway does not exist in solid-state synthesis.* Traditional solid-state synthetic techniques involve large diffusion distances in the initial reactants. Classic studies of bulk diffusion couples have shown that the growth of crystalline products rapidly becomes limited by the diffusion of the reactants through the product layer.[1] In this diffusion-limited regime, all stable phases found in the equilibrium phase diagram are formed as intermediates on the way to the final products. An example of this reaction is shown in Figure 1 for a molybdenum–selenium diffusion couple. The amount of each phase is determined by the relative diffusion rates of each atom through the various intermediate compounds.[2] A consequence of this bulk diffusion couple reaction is that only the most thermodynamically stable final products can be produced.

In contrast to bulk diffusion couples, kinetic evolution has been observed in diffusion couples, made by the sequential deposition of the reacting elements, whose layer thicknesses were several hundred angstroms.[1,3-8] As these diffusion couples are heated, a compound is observed to nucleate at the interface and grow until its growth exhausts one of the reactants.[9] Only then is another crystalline phase observed to nucleate at the compound–element interface.[10] The new compound grows until it exhausts either the supply of compound or element. This process repeats until the equilibrium mix of products is obtained. The sequence of phases formed on the way to this state depends upon the relative activation energies for nucleation of the various compounds. Compounds in the equilibrium phase diagram may be temporarily skipped if they have a large activation energy for nucleation. This reaction pathway is alternately limited by diffusion and nucleation, as illustrated in Figure 2.

There is a maximum thickness of the elemental layers which separates the above behavior from that observed in a bulk diffusion couple. This maximum thickness depends upon the rate of diffusion through the growing product layer and the activation energy necessary to nucleate a product at either of the compound–element interfaces. This behavior has been extensively investigated in metal–metal and metal–metalloid systems and the term "thin-film diffusion couple" has been coined to describe this thickness regime.

Although studies of thin-film diffusion couples have demonstrated a different and kinetically-controlled reaction mechanism, thin-film diffusion couples still do not permit control of the reaction intermediates. Conceptually, a solid-state reaction can be broken into two key steps: the interdiffusion of the reactants and the nucleation/crystallization of products. Thin-film diffusion couples are alternately limited by diffusion and nucleation. Any attempt to gain complete, kinetic control of the reaction pathway must be based upon eliminating diffusion as a rate-limiting step. This leaves nucleation, a kinetic phenomenon dependent upon overcoming a reaction barrier, as the crucial step to control.

A homogeneous, amorphous alloy is an ideal reaction intermediate for the preparation of extended solids. Long-range diffusion is completed in the formation of the alloy. This leaves nucleation as the rate-limiting step in the formation of a crystalline solid. Nucleation can be controlled by several strategies including impurities acting as nucleation seeds, using crystalline substrates

* Author to whom correspondence should be addressed.

(1) Gösele, U.; Tu, K. N. *J. Appl. Phys.* **1989**, *66*, 2619–2626.
(2) Brophy, J. H.; Rose, R. M.; Wulff, J. In *Thermodynamics of Structure*; John Wiley & Sons: New York, 1964; pp 91–94.
(3) Herd, S.; Tu, K. N.; Ahn, K. Y. *Appl. Phys. Lett.* **1983**, *42*, 597–599.
(4) Nava, F.; Psaras, P. A.; Takai, H.; Tu, K. N. *J. Appl. Phys.* **1986**, *59*, 2429–2438.
(5) Gas, P.; d'Heurle, F. M.; LeGoues, F. K.; La Placa, S. J. *J. Appl. Phys.* **1986**, *59*, 3458–3466.
(6) Coulman, B.; Chen, H. *J. Appl. Phys.* **1986**, *59*, 3467–3474.
(7) Clemens, B. M.; Buchholz, J. C. *Mater. Res. Soc. Symp. Proc.* **1985**, *37*, 559–564.
(8) Desrē, P. J.; Yavari, A. R. *Phys. Rev. Lett.* **1990**, *64*, 1533–1536.
(9) Walser, R. M.; Benē, R. W. *Appl. Phys. Lett.* **1976**, *28*, 624–625.
(10) Tsaur, B. Y.; Lau, S. S.; Mayer, J. W.; Nicolet, M.-A. *Appl. Phys. Lett.* **1981**, *38*, 922–924.

0002-7863/92/1514-4639$03.00/0